Technical Sciences, 2021, 24, 67–81

UNIWERSYTET WARMIŃSKO-MAZURSKI W OLSZTYNIE

Yearbook peer-reviewed scientific journal
ISSN 1505-4675
e-ISSN 2083-4527
TECHNICAL SCIENCES
Homepage: https://czasopisma.uwm.edu.pl/index.php/ts/

DOI: https://doi.org/10.31648/ts.6305

ANALYSIS OF A METHOD FOR MEASURING DEPOSIT IMPEDANCE PARAMETERS USING CHARGE AMPLIFIER AND LOCK-IN VOLTMETER

Dariusz Wiśniewski

ORCID: 0000-0001-8909-3159
Department of Electrical Engineering, Power Engineering, Electronics and Automation
University of Warmia and Mazury

Received 18 January 2021, accepted 10 August 2021, available online 13 August 2021.

K e y w o r d s: impedance, conductivity, moisture content, deposit, charge amplifier, lock-in voltmeter.

A b s t r a c t

Methods for measuring deposit parameters are often based on a capacitance or conductivity measurement aimed at estimating, e.g. deposit moisture content. In practice, these methods fail for materials with a low degree of homogeneity, a diverse porous structure or high conductivity, e.g. due to a high water content. This article demonstrates an approach that enables a more precise estimation of the parameters of any deposit. The presented method involves the use of a measuring system in a charge amplifier configuration and the application of a technique using lock-in detection or a lock-in voltmeter to determine resistance and capacitance parameters of a deposit based on signals received from the measuring system. This method can be successfully used wherever the test deposit material is highly heterogeneous and contains both dielectric and conductive materials. The article presents an example of a solution to a measuring system using two planar electrodes that can be dimensioned depending on the deposit dimensions. It is followed by a presentation of a method for converting the signal from the measuring system into impedance parameters of the deposit using a lock-in voltmeter. The analysis of the operation of the entire measuring system was modelled in Matlab/Simulink, and the operation results were presented.

Correspondence: Dariusz Wiśniewski, Katedra Elektrotechniki, Energetyki, Elektroniki i Automatyki, Uniwerssytet Warmińsko-Mazurski, ul. Oczapowskiego 11, 10-718 Olsztyn, phone: 89 523-43-64, e-mail: wdarek@uwm.edu.pl

Method for measuring deposit parameters

In this paper, methods for measuring deposit parameters are to be understood as electrical quantities that characterise a deposit, such as conductivity and capacitance. These quantities are often used for indirect measurement of other parameters, e.g. deposit material moisture content or bulk density or for spatial imaging.

A study by (FUCHS et al. 2008, TAN et al. 2017) presents a measurement of solid material deposit capacitance parameters taken to determine the moisture content. The measuring element applied was a sensor in the form of two planar electrodes. The test materials were pellets, homogeneously structured powders and plant materials. A different approach is presented in a study by (TAN et al. 2017), which examined the possibility for the use of deposit capacitance parameters to approximately determine the bulk density of miscanthus. In addition, the effects of the moisture content and particle size on the measurement results were investigated. An interesting application of capacitance parameters of a deposit is presented in a study by (AULEN, SHIPLEY 2012), where deposit capacitance parameters within the nanofarad range were used to assess the root system of crop plants.

Methods for measuring the impedance parameters of a deposit are also used in imaging techniques, e.g. electrical capacitance tomography (ECT) or electrical impedance tomography (EIT). Work in this area was performed in a study by WEGLEITER (2006). Capacitance tomography is also used in medical sciences. AMBIKA et al. (2019) used capacitance tomography to analyse bone density.

Fig. 1. An example of a deposit with a porous, heterogeneous structure

Capacitance tomography systems using methods which also enable impedance measurements were also demonstrated in a study by SMOLIK (2017). The methods presented in the study is based on the application of a lock-in amplifier as a method for measuring very low capacitances of the fF fraction order as well as impedance through the application of an additional reference signal.

This paper will focus on deposit material in the form of a thick, porous layer with a heterogeneous structure characterised by a significant gradient of moisture content changes in space. An example of such a deposit is presented in Figure 1.

Theoretical introduction

The method for measuring impedance parameters is based on the measurement of electrical conductivity and the capacitance of a deposit. It is assumed that the deposit will be placed in a reactor equipped with two parallelly arranged planar electrodes with a thin galvanic isolation layer. The system obtained in this way will be characterised by a certain capacitance of the order of single pF in the absence of a deposit and of the order of a maximum of several tens of pF in the presence of a very moist material. Conductivity between the electrodes will be strongly determined by the moisture content of the material placed between the electrodes. It was also assumed that the planar electrode surfaces had dimensions ensuring that electric field lines would penetrate through the largest possible cross-section of the deposit, which is aimed at ensuring the measurement of parameters for the largest possible volume of the test sample. Based on assumptions thus defined, the test system can be presented in the form of a planar loss capacitor with electrode surfaces S and the distance between them d. The system described in this way can be presented schematically, as in Figure 2.

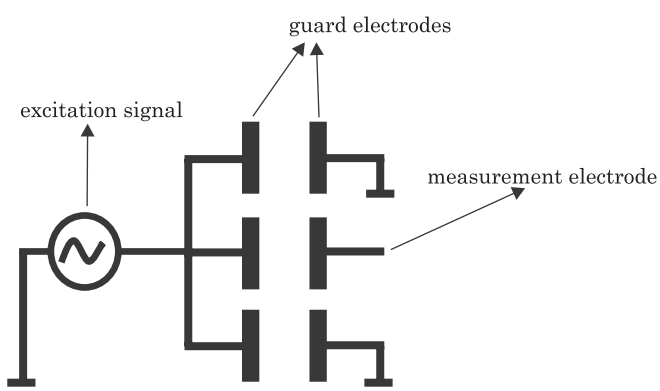

Fig. 2. A diagram of electrical connections of guard and measurement electrodes that neutralise field distortions

If there is air between the plates, the capacitor capacitance is described by the following relationship:

$$C = \frac{\varepsilon_o \varepsilon_r S}{d} = 8.854 \cdot 10^{-12} \frac{\varepsilon_r A}{d} \tag{1}$$

where:

ε_o – vacuum dielectric constant of $8.854 \cdot 10^{-12} \frac{\mathrm{F}}{\mathrm{m}}$,
ε_r – relative dielectric constant,
S – electrode surface [m^2],
d – distance between electrodes [m].

The relative dielectric constant for the air is 1.0006. Typical dielectric materials, e.g. plastic or oil, are characterised by a time-constant ranging from 3 to 10, while for polar fluids, e.g. water, the time-constant is 50 and more, depending on the temperature. Figure 3 presents the distribution of field force lines for a planar capacitor.

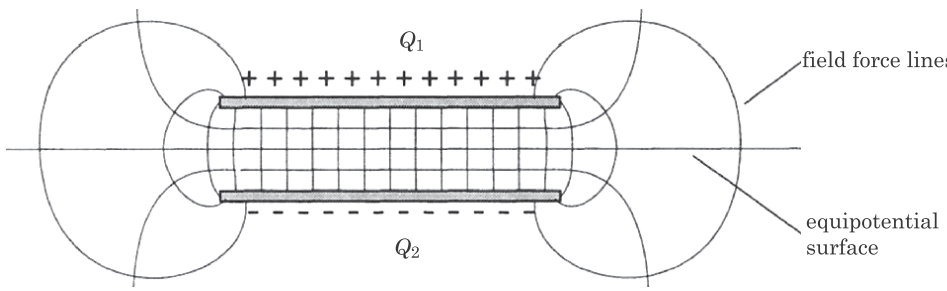

Fig. 3. Planar capacitor's field force lines
Source: based on BAXTER (1997).

Where the distances d for the electrodes are significant in relation to each other, in relation to plane A, the field lines at the planar capacitor electrode edges are arranged in semi-circles. This is such a strong phenomenon that formula (1) is only valid for small distances d between electrodes, such that the field lines are perpendicular to the electrode surfaces. For example, where the plates with a surface $S = 1\ \mathrm{m}^2$ are separated by a distance $d = 1$ mm, the planar capacitor capacitance is 88.54 pF, and is consistent with expression (1). Where the distance between electrodes is considerable, the so-called edge fields (which are not perpendicular in relation to the electrodes' internal surface) are formed at the electrode edges. Therefore, the capacitance between the electrodes can be considerably greater than that determined using formula (1). Figure 4 presents a distorted arrangement of the field lines at the electrode edges and a way to counteract this phenomenon.

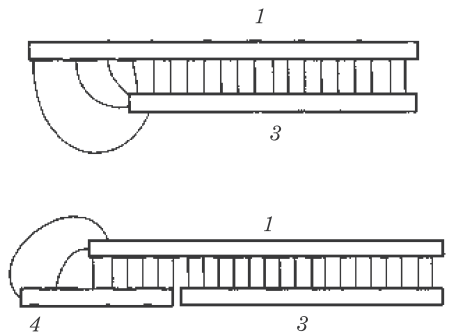

Fig. 4. The distribution of field lines at the electrode edges:
1, *3* – measurement electrode, *4* – guard electrode
Source: based on LARRY (1997).

The introduction of guard electrodes counteracts this phenomenon and brings the distorted field lines at the edges to the ground potential. Thanks to this solution, the distorted fields at the edges are insignificant for the measurement, and only the field lines that are perpendicular to the electrode plane play a role. Because of the application of guard electrodes, the distorted field lines generate a capacitance that is connected to the ground potential. Figure 2 presents an electrical diagram of connections that eliminates the impact of field distortions at the electrode edges on the measurement result.

The use of guard electrodes enables increasing the distance d of guard electrodes to a size allowing a porous deposit to be placed between the electrodes.

Measuring system

The system for measuring impedance parameters of a deposit needs to exhibit characteristics that will ensure the measurement of small values of the physical parameters between the measurement electrodes. It should be stressed that parasitic capacitances of the measuring circuits can be greater than the capacitance between the electrodes by an order of magnitude. The study adopted an electrode model using a loss capacitor with capacitance C and parallel resistance R_p. The electrode circuit model is shown in Figure 5.

For dielectrics such as plastics or ceramics, the loss factor D is relatively constant with an increase in frequency. On the other hand, for water, the loss factor D changes 4-fold with a change in frequency from 100 kHz to 1 MHz at a constant temperature of 25°C. Measurement of parameters for water below 100 kHz is difficult as the loss angle δ is almost 90°. At 100 kHz, the loss factor D amounts to 4, which means that the impedance angle is 76°, and the resistive element has a much lower impedance than that of the reactance element.

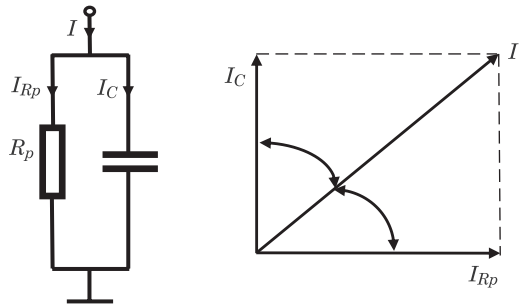

Fig. 5. A model of the measurement electrode circuit as a loss capacitor with capacitance C and loss resistance R_p. Phasor diagram of currents for the circuit

Figure 6 presents a diagram of changes in the relative permittivity ε_r and the dielectric loss factor D for water as a function of temperature for a frequency of 1 MHz (LARRY 1997).

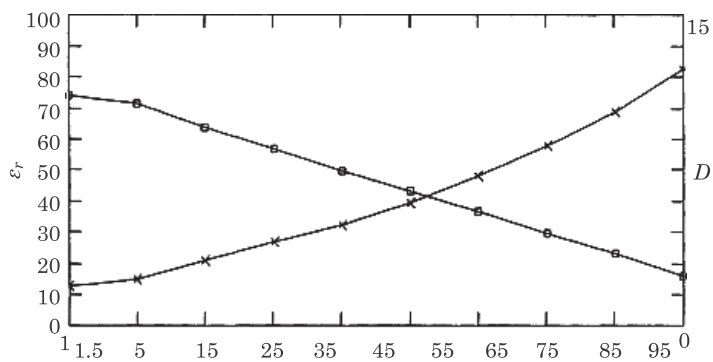

Fig. 6. A diagram of changes in the relative permittivity and the dielectric loss factor D for water as a function of temperature for a frequency of 1 MHz
Source: based on LARRY (1997).

Figure 7 shows that for materials containing water, the loss factor D is a more sensitive indicator than the relative permittivity ε_r. A change in water temperature from 15 to 75°C results in a 3-fold increase in the loss factor and a 2.5-fold decrease in the dielectric constant.

The design of the measuring system assumes the use of a two-electrode measuring element that will be subjected to sinusoidal excitations in order to obtain the best possible signal-to-noise ratio (ROFEE 1997). A basic diagram of the measuring transducer circuit is presented in Figure 8.

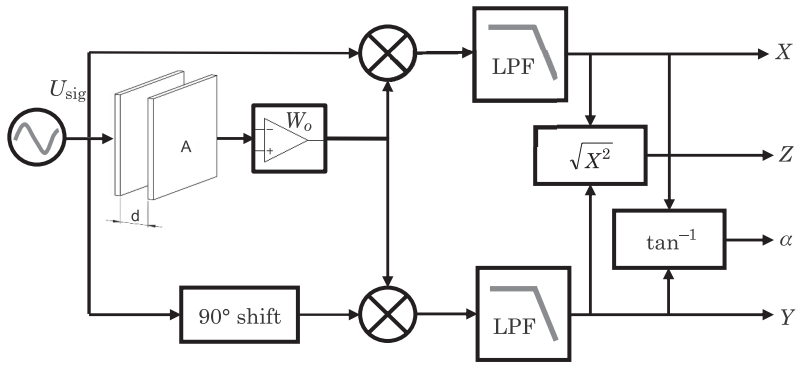

Fig. 7. Block diagram of the lock-in voltmeter circuit: X – real component, Y – imaginary component, Z – module, a – phase shift

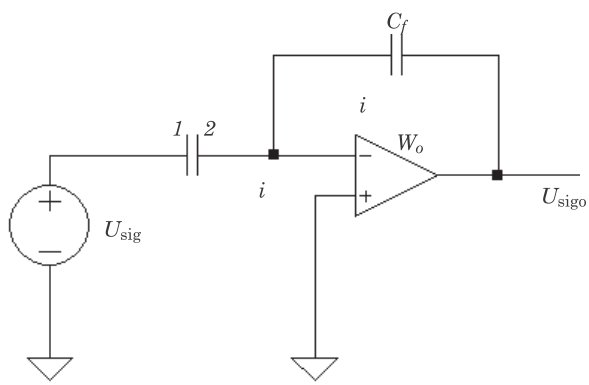

Fig. 8. Diagram of the measuring transducer circuit: *1* – excitation electrode, *2* – detection electrode

The basis measuring system comprises two planar electrodes #1 and #2, a source of a sinusoidal signal with low impedance, and an operational amplifier operating in an inverting configuration with capacitive feedback C_f. An excitation signal in the form of a sinusoidal wave is delivered to electrode #1

$$U_{\text{sig}} = U_a \sin(\omega_{\text{sig}} t) \tag{2}$$

while electrode #2 serves as a detection electrode. The signal in the form of an electric charge Q will be received from the detection probe and converted into a value proportional to charge Q_x transferred between the electrodes. The presented configuration is known in the literature as a charge amplifier and is widely used in applications in which the output signal is proportional to the electric charge. The relationship between the excitation signal and the output signal from the charge amplifier is described by the following relationship:

$$U_{\text{sigo}} = -\frac{C_x}{C_f} \cdot U_{\text{sig}} \tag{3}$$

where:

C_x – capacitance between the plates of electrodes #1 and #2 in [F],
C_f – capacitance of the charge amplifier feedback capacitor in [F],
U_{sig} – sinusoidal excitation signal,
U_{sigo} – sinusoidal output signal of the measuring transducer.

It follows from expression (3) that it is possible to easily determine the unknown capacitance C_x based on the parameters of the input signal, output signal and the known feedback capacitance C_f. The solution presented above is suitable for materials for which the conductivity between electrodes is negligibly low, i.e. of the order of μS. For conductive material, e.g. contaminated water, the situation changes, and conductivity has a greater influence on changes in the deposit impedance. Thus, a measuring transducer circuit in the form presented in Figure 9 is obtained.

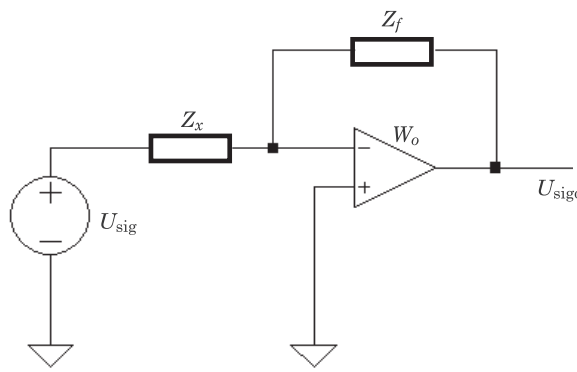

Fig. 9. A diagram of the measuring transducer circuit with a measurement electrode impedance model: Z_x – impedance of measurement electrodes, dependent on the deposit parameters, Z_f – feedback impedance of the operational amplifier

The transducer model shown in the figure can be described using equations in the complex form:

$$\underline{U}_{\text{sigo}} = \frac{\underline{Z}_x}{\underline{Z}_f} \underline{U}_{\text{sig}} \tag{4}$$

where:

Z_f – feedback impedance,
Z_x – sought impedance of measurement electrodes,
U_{sig} – sinusoidal excitation signal,
U_{sigo} – sinusoidal output signal of the measuring transducer.

It follows from equation (4) that the determination of unknown impedance Z_x requires knowledge of the parameters of the input signal, output signal, and the phase shift between these signals. The parameters of the input signal in relation to the output signal can be determined by the application of a lock-in voltmeter (SAIED 2016). The principle of operation of a lock-in voltmeter is shown in Figure 7. Excitation signal in the form of a sinusoidal wave:

$$U_{\text{sig}} = U_a \cdot \sin\left(\omega_{\text{sig}} t + \theta_{\text{sig}}\right) \tag{5}$$

where:

U_a – excitation signal amplitude,
ω_{sig} – excitation signal angular frequency,
θ_{sig} – excitation signal phase shift,
is introduced onto excitation electrode #1.

In accordance with the linear system theory, a signal with the same frequency ω_{sig} but with a changed amplitude U_{ao} and the angular shift of a will be obtained on detection electrode #2.

$$U_{\text{sigo}} = U_{ao} \cdot \sin\left(\omega_{\text{sig}} t + \theta_{\text{sig}} + a\right) \tag{6}$$

On the other hand, signals representing the real component X, imaginary component Y, module $|Z|$, and phase shift a will be obtained at the output of the lock-in voltmeter:

$$X = |Z| \cos\left(a\right) \tag{7}$$

$$Y = |Z| \sin\left(a\right) \tag{8}$$

$$|Z| = \frac{1}{2} U_a \cdot U_{ao} \tag{9}$$

$$a = \tan^{-1} \frac{Y}{X} \tag{10}$$

Based on the quantities obtained from the lock-in voltmeter and relationship (4), it is possible to determine the parameters of the sought impedance Z_x. Following the substitutions and conversions, the sought Z_x and its components are described with the following relationships:

$$\underline{Z_x} = \underline{Z_f} \frac{\underline{U_{\text{sig}}}}{\underline{U_{\text{sigo}}}} = |Z_f| e^{j\varphi_f} \cdot \left|\frac{U_a}{U_{ao}}\right| e^{-ja} \tag{11}$$

where:

$$U_{ao} = \frac{2 \cdot |Z|}{U_a} \tag{12}$$

$$\text{Re}\{Z_x\} = |Z_f| \cdot \left|\frac{U_a}{U_{ao}}\right| \cos\left(\varphi_f - a\right) = |Z| \cos(\varphi_f - a) \tag{13}$$

$$Im\{Z_x\} = |Z_f| \cdot \left|\frac{U_a}{U_{ao}}\right| \sin(\varphi_f - a) = |Z| \sin(\varphi_f - a) \tag{14}$$

$$X_{cx} = \sqrt{|Z|^2 \left(1 + \frac{1}{\mathrm{tg}(\varphi_f - a)^2}\right)} \tag{15}$$

$$R_x = X_{cx} \cdot \mathrm{tg}(\varphi_f - a) \tag{16}$$

$$C_x = \frac{1}{\omega_{\mathrm{sig}} X_{cx}} \tag{17}$$

Simulation model

Based on the analysis of the measuring system using a charge amplifier, and the analysis of lock-in voltmeter operation, a simulation model was constructed. The simulation model of the system was realised assuming ideal properties of the operational amplifier, i.e. an infinitely high gain in an open feedback loop, infinitely high input impedance, and infinitely wide transfer band. With these assumptions, equations 4 are true. A diagram of the model realised in Matlab/ Simulink is presented in Figure 10.

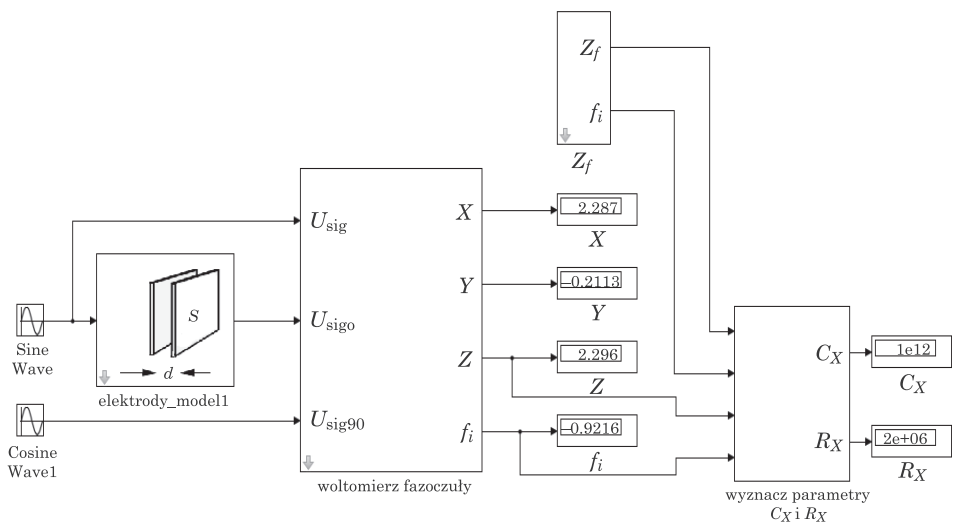

Fig. 10. A simulation model of the deposit impedance parameter measuring system

The simulation model comprises three independent blocks. The first block is responsible for simulations of the behaviour of measurement electrodes along with measuring transducer in accordance with equation (4) and the electrode model in the form of a loss capacitor with impedance Z_x. The second block simulates the operation of a lock-in voltmeter. In this block, synchronous detection and low-pass filtration occur, and the signal parameters in relation to the reference signal are then determined. The sinusoidal signal described by equation (5), which, at the same time, is the excitation signal of measurement electrode #1, was used as the reference signal. In a system with a single reference signal, it is possible to determine the amplitude U_{ao} of the test signal, which is received from measurement electrode #2. The determination of the phase shift between the reference signal and the test signal from detection electrode #2 requires the use of an additional reference signal phase-shifted by 90°. As a result of lock-in detection and the separation of the constant component using a third-order Butterworth low-pass filter with the corner frequency of 10 kHz, the parameters X, Y, $|Z|$ and a are obtained. The third block is used to determine impedance parameters of the test deposit according to equations (12)-(16).

Simulation testing was conducted for feedback parameters $C_f = 22$ pF and $R_f = 220$ kΩ. In practice, the feedback parameters should be set to the expected variability of the deposit parameters in order to obtain flat amplification characteristics over a wide frequency range. Figure 11 shows an example of the characteristics of the shift of a measuring transducer with ideal WO for the parameters shown in Table 1. It follows from the characteristics provided in Figure 11 that for the assumed feedback parameters, it is possible to obtain 3 dB a transfer band from a frequency of 200 krad/s.

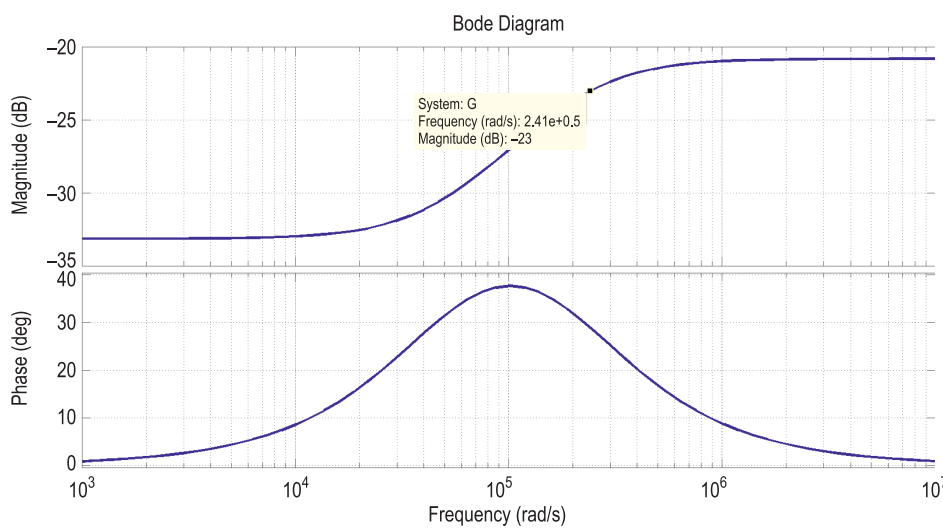

Fig. 11. Characteristics of the transfer of measuring transducer with ideal WO

Figure 12 shows a spectral analysis of the signal after the mixing of the signal received from the detection electrode with the reference signal. The spectrum has two characteristic peaks: the first one for the constant component, the second for the doubled frequency $2 \cdot \omega_{sig}$ of the excitation signal U_{sig}.

Table 1

Examples of feedback parameters Z_f of the operational amplifier

Parameter	R_f [MΩ]	C_f [pF]
Value	0.22	22

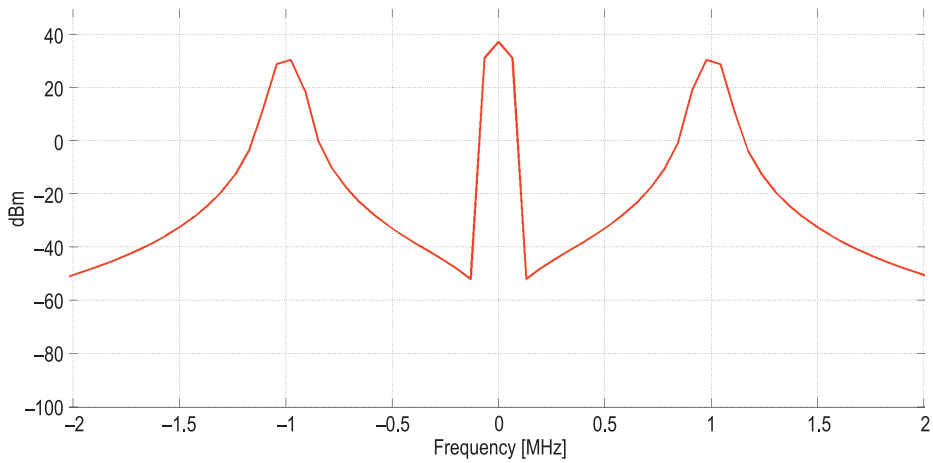

Fig. 12. The spectrum of the signal following the operation of multiplying the reference signal U_{sig} and the measurement signal U_{sigo}

The results of simulation testing of the system for measuring deposit parameters are presented in Tables 2 and 3. The simulation testing was conducted by setting capacitance C_x and resistance R_x that model the measurement electrodes, followed by simulations of the system with the parameters set.

Table 2

Examples of simulation results for the deposit impedance parameter measuring system at constant R_x=10 MΩ and the values of feedback elements C_f = 22 pF, R_f = 220 KΩ

Set value C_x [pF]	1	10	30	50
Determined value C_x' [pF]	1	10	30	50

Table 3

Examples of simulation results for the deposit impedance parameter measuring system at constant C_x=1 pF and the values of feedback elements C_f = 22 pF, R_f = 220 KΩ

Set value R_x [MΩ]	0.1	1	100	1000
Determined value R_x' [MΩ]	0.1	1	99.92	991.7

The obtained simulation data presented for the feedback values C_f = 22 pF and R_f = 220 KΩ ensure full compliance with the parameters set. Sensitivity S_x to a change in the charge between the electrodes of the testes measuring transducer is determined by feedback capacitance C_f. This is due to the fact that charge Q_x accumulated on measurement electrodes #1 and #2 is presented by the following expression:

$$Q_x = C_x \cdot U_{\text{sig}} \tag{18}$$

and, from relationships (3) and (18), sensitivity S_x to a change in the charge on measurement electrodes #1 and #2 amounts to:

$$S_x = \frac{U_{\text{sig}o}}{Q_x} = \frac{1}{C_f} = \frac{1}{22 \cdot 10^{-12}} = 0.0455 \left[\frac{\text{mV}}{\text{fC}}\right] \tag{19}$$

It is also possible to determine sensitivity S_c to a change in capacitance between the measuring transducer electrodes from equation (3). Assuming the excitation voltage amplitude U_a=10 V, the following capacitance sensitivity is obtained:

$$S_c = \frac{U_{\text{sig}o}}{C_x} = \frac{U_{\text{sig}}}{C_f} = \frac{10\ [\text{V}]}{22 \cdot 10^{-12}[\text{F}]} = 0.455 \left[\frac{\text{mV}}{\text{fF}}\right] \tag{20}$$

Obviously, the signal from the measuring transducer requires further amplification in real measuring systems, although this is not required for simulation purposes

Conclusions

The method for measuring impedance parameters of a deposit using a charge amplifier and a lock-in voltmeter allows very high accuracy to be achieved. The results of the simulation model testing lead to the conclusion that accuracy is limited only and exclusively by the accuracy of numerical methods of simulation programs. This is due to the fact that the process of determining impedance parameters in a numerical manner results directly from algebraic equations (7)-(17). A properly selected low-pass filter, which separates the constant component

from the variable component, which has a frequency twice as high as that of the excitation signal, guarantees accuracy arising directly from the numerical accuracy of algebraic transformations. The presented method ensures the certainty of the results obtained through simulation, but the situation is different as regards practical implementations. In practice, the process of detection from the detection electrode is affected by the influence of many interfering quantities, mainly in the form of parasitic capacitances of connections. These quantities are often higher by an order of magnitude than those being measured. Proper design of measuring circuits, shielding from external fields and proper design of guard electrodes will eliminate or significantly reduce their impact on the measurement process. As demonstrated using the examples of measuring transducer parameter values from relationship (20), it is possible to detect changes in capacitance on measurement electrodes of the femtofarad order. Methods using lock-in voltmeters are, due to their properties, often employed in many technical solutions, *inter alia* in capacitance tomography systems. The use of this method for measuring deposit impedance parameters will allow high accuracy to be achieved over a wide range of parameter changes. The practical implementation of a measuring system requires the preparation of measurement electrodes and their shielding and the selection of suitable electronic systems that ensure appropriate operation frequencies. The practical implementation can be carried out entirely using an analogue technique or partly using a digital technique.

References

AMBIKA M., MANIKANDAN K., PADMANABAN R. 2019. *Design and Fabrication of Electrical Capacitance Tomography Sensor with Signal Conditioning*. Biomed Research Journal BMRJ, 3(2): 79-85.

BAXTER L. 1997. *Capacitive Sensors. Design and Applications*. IEEE Press Series on Electronics Technology. Robert J. Herrick, Series Editor.

Characteristic and use charge amplifier. 2001. Technical information SD-37. Hamamatsu.

FUCHS A., ZANGL H., HOLLER G. 2008. *Capacitance-Based Sensing of Material Moisture in Bulk Solids: Applications and Restrictions*. Lecture Notes in Electrical Engineering, 20: 235-248.

KHOSHBAKHT M., LIN M. 2006. *Development of an electrical time domain reflectometry (ETDR) distributed moisture measurement technique for porous media*. Measurement Science and Technology, 17(11): 2989.

KRASZEWSKI A., TRABELSI S., NELSON S. 1999. *Moisture content determination in grain by measuring microwave parameters*. Measurement Science and Technology, 8(8): 857. DOI:10.1088/0957-0233/8/8/004.

MAURICE A., SHIPLEY B. 2012. *Non-destructive estimation of root mass using electrical capacitance on ten herbaceous species*. Plant and Soil, 355(1-2): 41-49. DOI:10.1007/s11104-011-1077-3.

ROFFE J. 1997. *A high-sensitivity flexible – excitation electrical capacitance tomography system*. Institute of Science and Technology, Manchester.

SAIED I., MERIBOUT M. 2016. *Electronic hardware design of electrical capacitance tomography systems*. In: *Philosophical Transactions of The Royal Society A Mathematical Physical and Engineering Sciences*. Royal Society. DOI: https://doi.org/10.1098/rsta.2015.0331.

SMOLIK W., KRYSZYN J., OLSZEWSKI T., SZABATIN R. 2017. *Methods of small capacitance measurement in electrical capacitance tomography*. Informatyka, Automatyka, Pomiary w Gospodarce i Ochronie Środowiska, 7(1): 105-110.

TAN Y., MIAO Z., ABDUL M., GRIFT T., TING K. 2017. *Electrical capacitance as a proxy measurement of miscanthus bulk density, and the influence of moisture content and particle size*. Computers and Electronics in Agriculture, 134: 102–108.

TOMKIEWICZ D. 2009. *Budowa i działanie czujnika wilgotności ziarna zboża wykorzystującego promieniowanie w zakresie bliskiej podczerwieni*. Inżynieria Rolnicza, 6(115).

WEGLEITER H. 2006. *Low-Z Carrier Frequency Front-End for Electrical Capacitance Tomography Applications*. Dissertation. Graz University of Technology, Austria.

WOBSCHALL D., LAKSHMANAN D. 2005. *Wireless soil moisture sensor based on fringing capacitance*. Proc. of IEEE Sensors, p. 8–11.

WYPYCH P. 2001. *Dilute-phase pneumatic conveying problems and solutions*. In: *Handbook of Conveying and Handling of Particulate Solids*. Eds. A. Levy, H. Kalman. Elsevier Science, Amsterdam, p. 303–318.

YANG W.Q. 1996. *Hardware design of electrical capacitance tomography systems*. Meas. Sci. Technol., 7: 225–232.

YANG W.Q., STOTT A.L., BECK M.S., XIE C.G. 1995. *Development of capacitance tomographic imaging systems for oil pipeline measurements*. Rev. Sci. Instrum., 66: 4326–4332.

YANG W.Q., YORK T.A. 1999. *New AC – based capacitance tomography system*. IEE Proc-Sci. Measurement Technology, 146(1): 47–53.